The Interaction of Water with the Pt(533) Surface

Mihail L. Grecea,*,§ Ellen H. G. Backus,§ Bernd Riedmüller,§ Andreas Eichler,|| Aart W. Kleyn,§,‡ and Mischa Bonn§,†

Leiden Institute of Chemistry, University of Leiden, Einsteinweg 55, P.O. Box 9502, 2300 RA Leiden, The Netherlands, Institute of Material Science and Center for Computational Materials Science, University of Vienna, Sensengasse 8/12, 1090 Vienna, Austria, FOM Institute for Plasma Physics Rijnhuizen, Euratom-FOM Association, P.O. Box 1207, 3430 BE Nieuwegein, The Netherlands, and FOM Institute for Atomic and Molecular Physics AMOLF, Kruislaan 407, 1098 SJ Amsterdam, The Netherlands

Received: February 10, 2004; In Final Form: June 8, 2004

The adsorption of water on the stepped Pt(533) surface has been investigated using temperature-programmed desorption (TPD) and reflection absorption infrared spectroscopy (RAIRS). Both the TPD spectra and the RAIRS results reveal two submonolayer states and one multilayer phase. In the submonolayer regime, water first adsorbs on the Pt(100)-step edges of the surface. The water molecules at these steps induce a supplementary stabilization of the water that subsequently adsorbs onto the four atoms wide (111) terraces. In contrast, the multilayer TPD feature is not affected by the stepped nature of the substrate and is very similar to water desorption from, for example, the flat Pt(111) surface. RAIRS data indicate strong hydrogen-bonding interactions between water molecules adsorbed on the steps already at very low coverages ($\leq$0.13 ML). This is in agreement with DFT calculations that demonstrate that the water−water interaction is sufficiently strong that water molecular chains could be formed along the step edges at very low coverage. Both the RAIRS data and the DFT calculations support intact H_2O adsorption on Pt(533).

1. Introduction

Knowledge concerning the interfacial water structure at metal surfaces is crucial for the understanding of many important surface phenomena involving water in, for example, electrochemistry, corrosion processes, and the photocatalytic decomposition of water as a renewable energy source. Studies of the interaction of water with single-crystal transition-metal surfaces have revealed a rich behavior, on which recent reviews[1,2] provide ample background. However, even on well-defined single-crystal metal surfaces the structure and composition of adsorbed water layers still raise controversies, for instance, in the interaction of water with "nonreactive" metal surfaces (such as Pt, Pd, Rh, Ru).[3] Most of the investigations so far have shown that these metal surfaces do not (significantly) dissociate water,[1,4] although recent calculations[5,6] and experiments[7] have indicated that for water on Ru(0001) a partial dissociated water layer may be energetically most favorable. For water on Pt(111), there has been some debate regarding the atomic roughness of the first layer, the nature of water bonding to Pt atoms, and the presence of free OH groups.[8,9]

On the Pt(111) surface, adsorption of both H_2O and D_2O has been studied by a large number of techniques.[8,10−23] Water adsorbs *molecularly* at all coverages, as has been concluded from X-ray photoemission spectroscopy (XPS), ultraviolet photoemission spectroscopy (UPS),[10] and high-resolution electron energy loss spectroscopy (HREELS).[17] No isotope (Ubbelhode) effect[22] in H_2O/D_2O desorption from Pt(111) has been observed in temperature-programmed desorption (TPD)[11] and high-resolution helium atom diffraction (HAD)[23] investigations. Water adsorption on the Pt(111) surface at 80−135 K has been traditionally reported to result in an ice-like bilayer consisting of puckered rings of water hexamers with long-range order.[20,23,24] However, after annealing of a water multilayer on Pt(111) at 140 K, a more planar adsorption state at 110−120 K was recently reported on the basis of X-ray measurements and theoretical calculations.[8]

The lateral H-bonding interaction of water molecules on the Pt surface is present already at the initial stages of adsorption—even at very low surface temperatures (0.015−0.105 monolayers at 20 K[15] or 0.027 monolayers at 60 K[19]). The hydrogen bond energy ($\sim$39 kJ/mol for water dimers and $\sim$44 kJ/mol in bulk ice[23]) is comparable to the water−Pt(111) binding energy ($\sim$40 kJ/mol).[2,21,23] Hydrogen bonding was also evidenced by HREELS measurements in the submonolayer regime, by a continuous red shift of 50−70 cm^{-1} of the O−H stretch vibration with increasing coverage.[17,18] Recent experiments of low-energy H^+ scattering emphasized the considerably covalent character of hydrogen bonds within water structures formed on Pt(111).[25]

One TPD peak has been reported recently for water adsorbed in the submonolayer regime on Pt(111), at various adsorption temperatures of 85−137 K and for heating rates of 0.6−4 Ks^{-1}.[12,13,24,26−28] Water desorption from a flat Pt(100) surface was reported as occurring around 168 K, at very high heating rates (12−16 Ks^{-1}).[29,30] One TPD peak, at 150−160 K, has been also observed for multilayer desorption in several studies on Pt(111).[11−13,24,26,27]

Although a large number of studies have focused on the behavior of water on atomically flat Pt, Pd, Rh, and Ru surfaces,[1,2,5,10−17] there are only few reports of water on well-defined stepped metal surfaces: these are limited to the

* Corresponding author. E-mail: m.grecea@chem.leidenuniv.nl; phone: +31-71-5274452; fax: +31−71−5274451.
§ University of Leiden.
|| University of Vienna.
‡ FOM Institute for Plasma Physics Rijnhuizen.
† FOM Institute for Atomic and Molecular Physics AMOLF.

10.1021/jp049392c CCC: $27.50
Published on Web 07/27/2004

Ru(10$\bar{1}$*N*), with $N = 8, 12, 22$,[31,32] Pt(755),[33] and Pt(335) surfaces[34] (Pt(335) and Pt(533) indicate the same surface structure, consisting of four atoms wide Pt(111) terraces and one atom wide Pt(100) steps; we will use the (533) notation here). For the Ru stepped surfaces, the steps resulted in an additional TPD peak at high temperatures, thought to be due to a partial dissociation of water at the step sites. The TPD spectra of the first water layer adsorbed on the Pt(533) surface[34] show a high-temperature shift of 25−35 K, in comparison with the Pt(111) surface.[12] Moreover, alloying the Pt(111) surface with Sn, which leads to poisoning of defect-related step sites, results in disappearance of the high-temperature shoulder believed to be related to desorption of water from step defects.[12] In addition, variable temperature scanning tunneling microscopy (STM) measurements suggested that the desorption temperature of a water submonolayer from terrace sites differs from desorption from the steps generated previously by ion bombardment of a Pt(111) surface.[1,21] UPS results indicate the adsorption of the *molecular* H_2O on the Pt(755) surface, although no information concerning the nature of water at steps has been offered.[33]

In addition to the precise role of the steps in the interaction of water with the stepped Pt surface, the sticking probability of water molecules on this surface, the influence of hydrogen bonds and the long-range order within water structures developed under various adsorption conditions as well as the nature of water multilayers grown on a Pt(533) surface have remained largely unexplored.

In this study, we report on the adsorption behavior of water on a stepped Pt(533) surface, using TPD and reflection absorption infrared spectroscopy (RAIRS). We present TPD spectra of water submonolayers and multilayers adsorbed on Pt(533) at 100 K, measured at various heating rates ($2-6\ Ks^{-1}$). Coadsorption experiments of H_2O combined with CO have been performed to investigate the interaction between water on the steps and water on the terraces. The sticking coefficient of water on an incompletely water-covered Pt surface and also on water ice multilayer is obtained from an uptake curve of integrated TPD spectra. The study was complemented by RAIRS investigations of several submonolayer and (amorphous and crystalline) multilayers of water adsorbed on the Pt(533) surface. DFT calculations of adsorption configurations and energetics complete the study of submonolayer water adsorbed on the Pt(533) surface. We clearly observed that the higher coordination offered by the (100) step sites leads to more strongly bound water, compared to atomically flat (111) terraces.[12,13] In addition, we observe that these step-bound water molecules stabilize water molecules that are subsequently adsorbed on the flat (111) terraces; there is a marked influence of water−water interactions on desorption from a Pt(533) surface. Both RAIRS data and DFT calculations suggest that water adsorbs intact on Pt(533).

2. Setup and Method

2.1. Experimental. The experiments were performed in an UHV chamber (with a base pressure of 3×10^{-11} mbar) that has been described in detail elsewhere,[35,36] with a triply differentially pumped, compact molecular beam line for water dosing. The Pt(533) sample was cleaned by repeated cycles of Ar^+ sputtering at 298 K, oxygen treatment (5×10^{-7} mbar) between 750 and 970 K, and annealing at 1270 K. The long-range order and cleanliness of the surface were checked by low-energy electron diffraction (LEED, VG Microtech) and by comparison of nitrogen oxide TPD spectra with previous reports.[37] Every experimental session was preceded by 40 min of sputtering with subsequent annealing at 1270 K.

The water dosing beam line consists of three different pumping stages to ensure an optimal pressure gradient required for a controllable flux and a reproducible water molecular beam. Water was obtained from a Simplicity Millipore system (resistivity value >18 MΩ/cm). A variable beam flux between 0.01 and 0.06 MLs^{-1} was used to grow water layers on the Pt surface at temperatures of 100 K. The flux of the water beam was controlled by varying the expansion pressure of the water vapor. The diameter of the molecular beam at the crystal position exceeds that of the crystal, so that a uniform layer is deposited.

To record TPD spectra, the crystal was placed 5 mm from the shield of a differentially pumped quadrupole mass spectrometer (QMS, Balzers QS 422), in a collinear geometry with the ionizer. Water is detected at $m/z = 18$. Various heating rates ($2-6\ Ks^{-1}$) were employed. The RAIRS spectra were recorded at 4 cm^{-1} resolution with a Fourier transform infrared (FTIR) spectrometer (Biorad FTS 175) connected to an external liquid nitrogen cooled mercury−cadmium−telluride (MCT) detector. The infrared light was incident upon the crystal at an angle of 85° with respect to the surface normal.

In this study, a ML (monolayer) is defined as the amount of water necessary to form an ice-like bilayer on the substrate. It is equivalent to the term bilayer (BL) and is defined as the coverage for which the ∼198 K TPD signal is saturated and the multilayer peak at 160 K starts to appear.[38] The water coverage was determined from the integrated area under the TPD peaks, while the CO exposure is given in langmuirs (1 langmuir (L): 1×10^{-6} mbar s). The reported pressures are not corrected for ion-gauge sensitivity.

2.2. Calculation. Structures and binding energies have been calculated using the Vienna Ab-initio Simulation Package (VASP).[39−41] VASP is a plane wave based density functional code employing the projector augmented wave method.[42] The surface has been modeled by a 19 layer slab in a 4×1 cell containing 4 atoms per layer, sampled by a grid of $(3 \times 2 \times 1)$ k-points. A cutoff energy for the expansion of the plane waves of 400 eV was sufficient for an accurate description. To account for exchange and correlation effects, generalized gradient corrections (GGA) according to Perdew et al.[43] have been applied. The adsorption energies were corrected by the appropriate zero point energies, calculated from the vibrational spectra obtained by diagonalization of the dynamical matrix from finite displacements ($\Delta = \pm 0.02$ Å) of every ion of the water molecule into each Cartesian coordinate.

3. Results and Discussions

3.1. The Submonolayer Regime. TPD spectra (heating rate: $2\ Ks^{-1}$) for submonolayer coverages (dosed at $T = 100$ K) are shown in Figure 1 (top panel). For very low exposures (corresponding to coverages $\Theta \leq 0.13$ ML), we observe one peak which shifts from 194 to 198 K with increasing exposure and then remains at a constant position (∼198 K). For coverages exceeding $\Theta \sim 0.33$ ML, a shoulder appears in the TPD spectra at 185 K. When the coverage exceeds $\Theta = 1.0$ ML, these two peaks saturate and a multilayer peak at ∼160 K appears (as illustrated by the 1.08 ML experiment). These observations are summarized in Figure 1 (middle panel), depicting the total TPD intensity and the relative magnitude of the two contributions (obtained by Gaussian fits to the data, as illustrated in the inset of Figure 1 (middle panel)) as a function of exposure. The linear behavior, with increasing exposure, of the total amount of water desorbed from the Pt(533) surface indicates a coverage-independent sticking coefficient (S) of water molecules in the submonolayer regime. In addition, as shown in Figure 1 (bottom

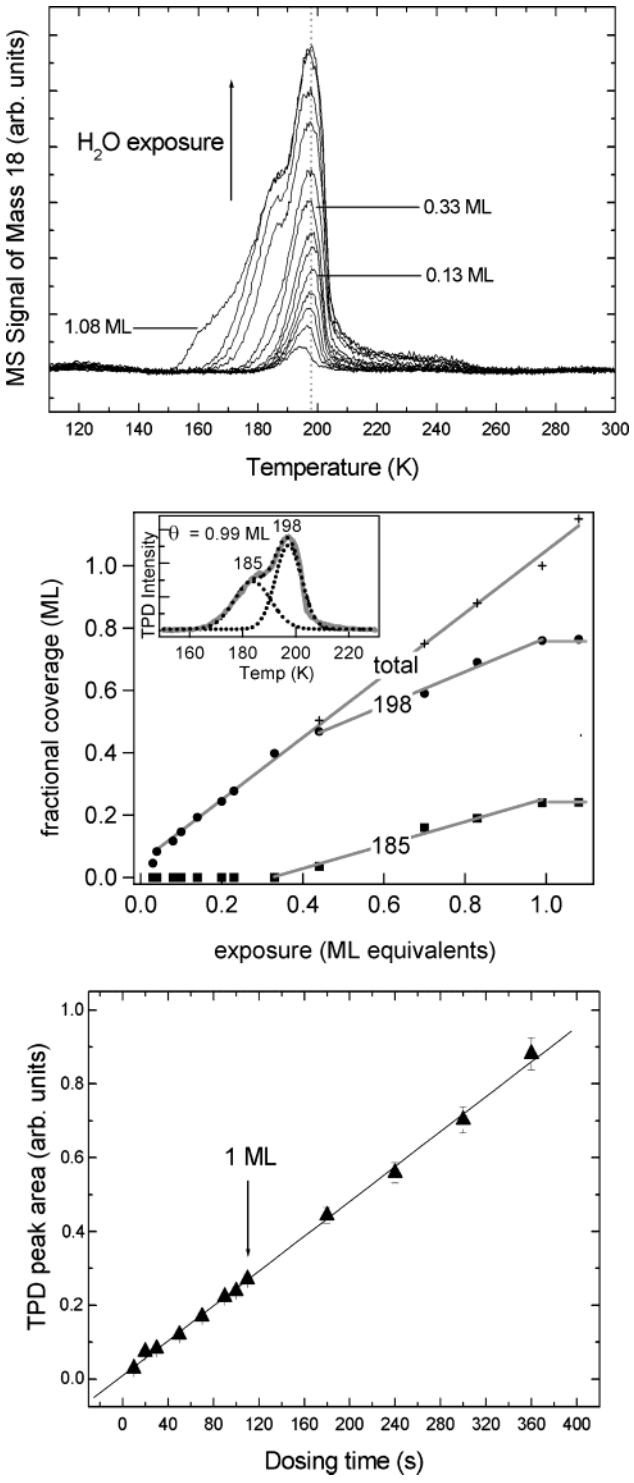

Figure 1. Top panel: TPD spectra of H_2O dosed at $T_S = 100$ K on Pt(533). Left axis: mass spectrometer (MS) signal at $m/z = 18$. Water dosing rate was 0.01 MLs^{-1}; the (submonolayer) coverages (in ML, computed on the basis of peak integrated areas) are, from bottom to top, 0.03, 0.06, 0.08, 0.10, 0.13, 0.20, 0.23, 0.33, 0.44, 0.70, 0.83, 0.99, and 1.08. The heating rate was 2 Ks^{-1}. Middle panel: H_2O uptake curves, determined from the integrated areas of the TPD curves presented in Figure 1a (+), as well as the individual contributions at 185 K (■) and 198 K (●) obtained from Gaussian fits, in the submonolayer regime of water on Pt(533), as illustrated in the inset for one monolayer coverage. The residual coverage at zero exposure is due to small amounts of water in the background. Bottom panel: H_2O uptake curve on the Pt(533) surface for an adsorption (surface) temperature of 100 K, determined from the integrated areas of the TPD curves such as those presented in Figure 1a.

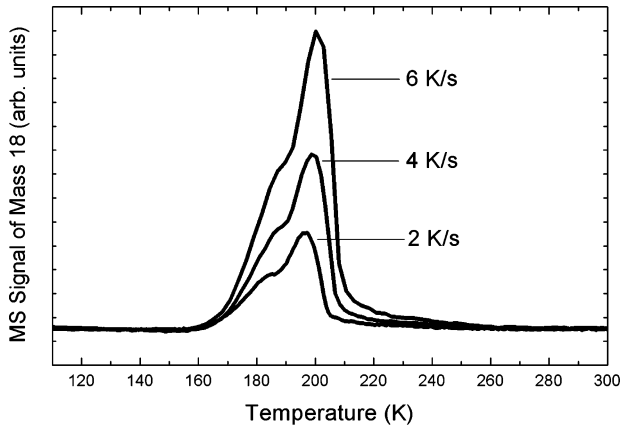

Figure 2. TPD spectra of H_2O dosed (under similar conditions of expansion pressure and dosing time) on Pt(533) at 100 K (corresponding to a coverage of 0.7 ML). Left axis: mass spectrometer (MS) signal at $m/z = 18$. Heating rates were 2, 4, and 6 Ks^{-1}. The increased MS signal for higher heating rates is because the MS signal is proportional to the desorption rate, which, in turn, scales with the heating rate; although the total amount of desorbed water is identical for the three measurements, the signals scale by the relative ramp rates.

panel), the slope of the uptake curve at 100 K in the submonolayer regime is identical to that in the multilayer regime (obtained from TPD spectra of water multilayers shown below, in Figure 7), where the sticking coefficient has been reported to be close to unity at 100 K.[44−46] Thus, we conclude that, within the experimental error of ∼5%, the sticking coefficient S equals 1 for water on the Pt(533) surface.

Previous experiments of water desorption from the Pt(533) surface[34] have not reported the double-peak structure at 195 K. This is presumably caused by the high heating rates used in those experiments.[34]

It has been suggested that a rearrangement of water molecules on the Pt surface occurs during the TPD measurement.[16] This rearrangement resulted in the observation of heating rate-dependent TPD spectra. We do not find evidence for this phenomenon on the Pt(533) surface, as illustrated in Figure 2. The TPD features observed here seemingly originate from the various adsorption/desorption sites of the Pt(533) surface, which apparently are different from those of flat Pt(111)[12,13,24,26−28] (Table 1) and Pt(100)[29,30] surfaces.

The desorption temperatures observed here for Pt(533), 185 and 198 K, are relatively high compared to the (111) surface. This can be understood for desorption from the steps, as one would expect stronger interaction at those sites, but for desorption from the terraces one might expect a desorption temperature similar to that from the flat Pt(111) surface. Indeed, as shown in Figure 3, upon blocking the (100) step sites with CO (2.5 L dosed at 440 K, prior to water dosing at 100 K),[47−50] desorption of water adsorbed only on the (111) terrace sites of Pt(533) surface occurs around 175 K (dashed curve), with a single TPD peak, which is very similar to the desorption of water from bare Pt(111).[11,13,26] This lower desorption temperature can be attributed to a weaker binding of water on the terrace site in absence of water on the step sites. The temperature shift is not caused by a local modification of the electronic structure upon CO adsorption (as previously observed for Pt(111)[51]), as is apparent from the observation that partial (∼40%) blocking of step sites by CO leads to only a very small shift (2−3 K) of the water desorption temperature (Figure 3, gray curve). From this, we conclude that the effect of coadsorbed CO on further H_2O adsorption on Pt(533) appears to be steric

TABLE 1: Summary of TPD Features of Water on Pt(111) and Pt Stepped Surfaces Reported Previously

surface	Pt(111)						Pt(335)[b]	Pt(533)
monolayer (K)	163−167	171	168	176−180	160−165	157−167	195	194−198 185
multilayer (K)	161→[a]	154	155	161	150		155→[a]	160→[a]
heating rate (Ks^{-1})	4	3	0.65	1	1	0.6	10	2-6
adsorption (surface) temperature (K)	100	137	137	85	85	100		100
reference	12	13	24	26	27	28	34	this work

[a] →: shifting to higher *T* as coverage increases. [b] The Pt(335) and Pt(533) surfaces both consist of four atoms wide Pt(111) terraces separated by one atom wide Pt(100) steps.

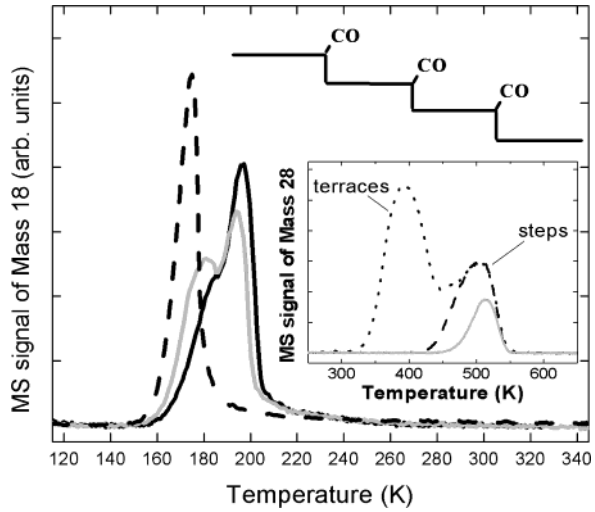

Figure 3. TPD spectra of H_2O submonolayer dosed at 100 K on 2.5 L of CO preadsorbed at 440 K on the Pt(533) surface (dashed curve) and 0.1 L of CO preadsorbed at 440 K on the Pt(533) surface (gray curve) and on the bare Pt(533) surface (continuous curve), respectively. Water dosing rate was 0.01 MLs^{-1}. Heating rate was 2 Ks^{-1}. Inset: (upper) schematic diagram of the CO presaturated steps of the Pt(533) surface; (bottom) TPD spectra of 2.5 L of CO dosed at 440 K on the Pt(533) surface corresponding to full saturation of the step sites (dashed curve) and, respectively, 0.1 L of CO dosed at 440 K for partial saturation (∼40%, as resulted from the integrated TPD peak area) of the step sites (gray curve); for comparison, the TPD spectrum of the fully CO-covered Pt(533) surface is also shown (dotted curve).

rather than electronic. Preadsorbed CO simply blocks the step sites and thereby indirectly affects the adsorption of water on the terrace sites. The effect of the (100) steps on the Pt(533) surface structure therefore appears to consist of a stabilization of water molecules adsorbed on the (111) terrace sites of the Pt(533) surface. This explains the higher desorption temperature (∼185 K) observed in the submonolayer regime (Figure 1 (top panel)) compared to water desorption temperatures (163−178 K) observed for Pt(111).[11−13]

To further corroborate these findings, we also investigated the nature of thin water films grown on the Pt(533) surface by RAIRS. Figure 4 (left panel) depicts RAIR spectra in the frequency range of 3000−3520 cm^{-1} of water adsorbed in the submonolayer regime on the Pt(533) surface, at coverages of 0.05, 0.13, 0.33, 0.39, 0.51, 1.0 ML (lines a−f, respectively). Water was dosed at 100 K, while the RAIR spectra were recorded at 85 K.

The most striking feature in the spectra shown in Figure 4 (left panel) is the presence of the narrow peak at ∼3318 cm^{-1} already at the lowest coverage (0.05−0.13 ML). The spectral band in this range (3290−3450 cm^{-1}) reflects an OH stretching vibration[1,2] and has been reported as characteristic for the hydrogen bonded O−H···O bond,[52,53] indicating that hydrogen bonding occurs already at very low water coverages (vibrational frequencies associated with H_2O monomers are expected at higher values (∼3700 cm^{-1}), nearer to the gas-phase values,[54] and are not observed in our experiments in the submonolayer regime). This is consistent with previous reports of water clustering on Pt at very low coverages (<0.1 ML) at temperatures around 20−60 K[15,16,19,24] and also is in agreement with the observed frequency of 3334 cm^{-1} for water adsorbed on Pt(111),[14] recently interpreted as chains along the step edges.[18] However, the OH stretching frequency at low coverages on the Pt(533) surface (3318 cm^{-1}) is significantly lower than that reported for the (100)[30] and (111)[53] surfaces, for which a frequency of ∼3430 cm^{-1} has been observed with HREEL spectroscopy. This indicates that the hydrogen-bonding interaction on the stepped surface is markedly stronger than that on the flat surfaces.

The intensity of the peak at 3318 cm^{-1} increases as the submonolayer coverage increases, but initially retains its shape (Figure 4 (left panel), curves a−d). Subsequently, a shoulder develops at higher frequencies and a broadening is visible at coverages >0.39 ML (curves e−f). This roughly corresponds to the coverage where the additional peak in the TPD spectra appears.

As the peak at 3318 cm^{-1} is not observed for dissociated water on Ru(0001)[7] and for the mixed ($OH+H_2O$) phase on Pt(111),[55] the appearance of this peak (Figure 4 (left panel)) is a strong indication for the adsorption of intact water. This interpretation is also corroborated by evaluating the integrated RAIRS signal in the ∼3300 cm^{-1} region versus water submonolayer coverage, plotted in Figure 4 (right panel). This H_2O stretching peak is suppressed in the IR spectrum of the mixed ($OH+H_2O$) phase owing to the nearly flat, dipole inactive geometry of water in this mixed structure.[56] As the linear fit through the data has zero intensity at zero coverage (Figure 4 (right panel)), we can conclude that water adsorbs intact on the Pt(533) surface.

By combining the RAIRS data, which suggest that hydrogen bonding occurs already at 0.05 ML coverage as well as that water adsorbs intact on Pt(533), and the TPD data, suggesting preferential occupation of the step sites at low coverage, our results indicate that for very low coverages (<0.13 ML) intact adsorbed water forms molecular chains on the steps of the Pt(533) surface. This interpretation is consistent with previous observations of one-dimensional growth of water molecular arrays along the (defect-related) step edges on the Pt(111) surface, using HREELS[18] and STM techniques.[21] The preferential occupation of the step edges is a consequence of the strong interaction of water with step sites (the Smoluchowski effect)[1,21,57] and the mobility of water on the Pt surface already at 100 K.[1,16] At this temperature, the surface (electronic or physical) corrugation is insufficient to inhibit surface diffusion. As the water−Pt interaction is comparable with the water−water interaction,[21,23,58] clustering of water molecules is facile.[1]

The preference of water for intact adsorption on the step sites of the Pt(533) surface is corroborated by adsorption energies

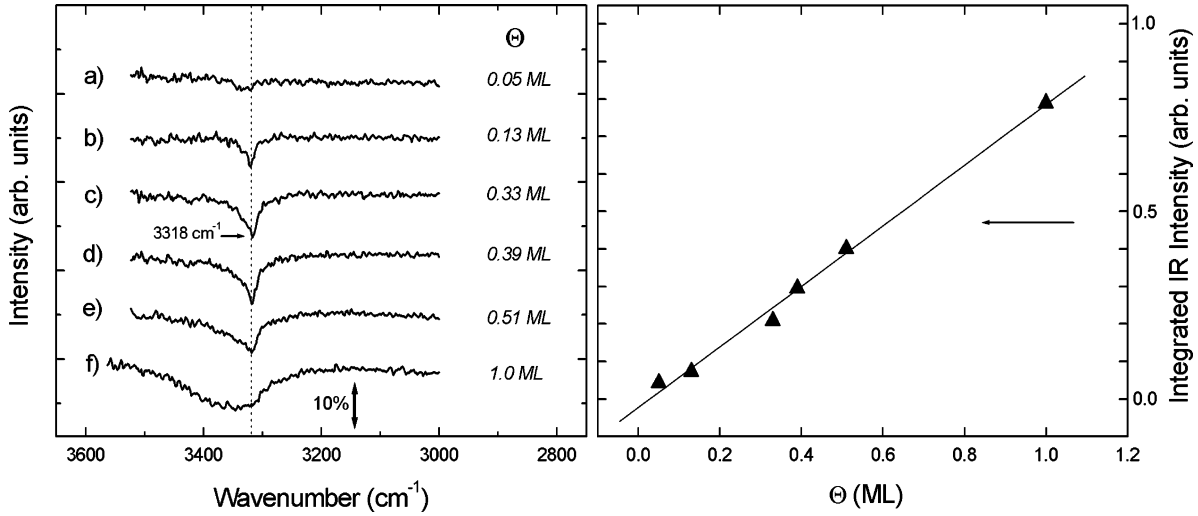

Figure 4. Left panel: RAIR spectra for submonolayers of H_2O adsorbed on Pt(533), shown in the frequency range of 3520−3000 cm^{-1}. The amount of water corresponds to coverages of 0.05 ML (a), 0.13 ML (b), 0.33 ML (c), 0.39 ML (d), 0.51 ML (e), and 1.0 ML (f), respectively. The water coverage was determined from the integrated area of the corresponding TPD spectra. Right panel: Integrated intensity of the IR absorption around 3300 cm^{-1} (curves a−f) as a function of the H_2O coverage. The linear fit through the data has zero intensity at zero coverage indicating, within experimental error, that water adsorbs intact on the Pt(533) surface.

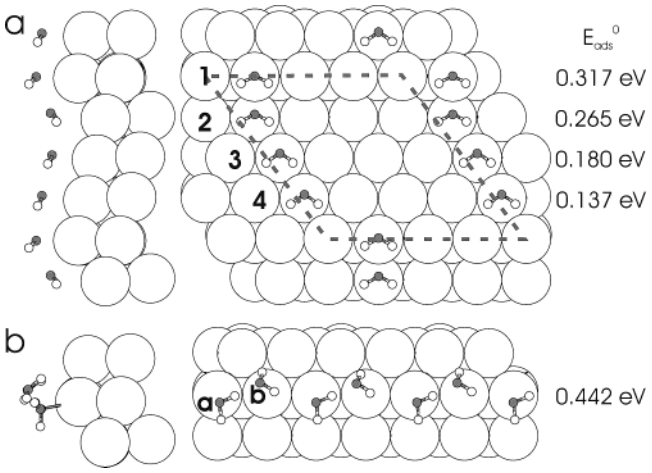

Figure 5. (a) Side and top view of the atop adsorption sites of the H_2O monomer on the Pt(533) surface. The side view is restricted to the uppermost two layers only. In the top view, a dashed gray line indicates the unit cell used for the calculation. (b) Side and top view of H_2O molecular chains adsorbed on the step sites of the Pt(533) surface. Adsorption energies per molecule including zero-point corrections (E_{ads}^0) are also presented. All DFT calculated adsorption energies and geometries are presented in Table 2.

obtained from DFT calculations. Figure 5a illustrates the different (atop) adsorption sites available for a water monomer on the Pt(533) surface and the corresponding adsorption energies (including zero-point corrections), E_{ads}^0. All the associated adsorption energies as well as the parameters characterizing the adsorption geometry are given in Table 2. (The atop site has been previously indicated as the preferred adsorption site for H_2O on transition metals[2,59−61]). Clearly, a tendency for stronger binding in the vicinity of the upper step edge (adsorption site 1 in Figure 5a) can be seen from the adsorption energies, as well as from the adsorption height (d_{Pt-O}). For this site, the adsorption energy is much higher than in the middle of the terrace (site 3 in Figure 5a), where the adsorption behavior is similar to the flat Pt(111) surface (cf. Table 2). The opening angle and O−H distances are very similar for all adsorption sites and close to the corresponding gas-phase values; only the adsorption site at the lower step edge leads to a substantial distortion of the molecule. Here, the dominant attraction toward the upper step edge tilts the molecule such that in the equilibrium position, the oxygen atom is closer to the Pt atom of the upper step edge than to that in the terrace below.

To explore the possibility of dissociation, we did a similar adsorption study for the fragments resulting after dissociation, the hydroxyl group (OH) and the hydrogen atom (H). For both adsorbates, the ontop adsorption site was chosen, which is the equilibrium adsorption site for OH and only slightly less stable (∼0.1 eV) than adsorption in fcc hollow sites for H.[62] Either of the adsorbates was adsorbed individually at the surface, adsorption energies together with some parameters characterizing the

TABLE 2: Adsorption Energies Per Molecule without (E_{ads}) and with Zero-Point Corrections (E_{ads}^0) Together with Geometrical Parameters for a H_2O Monomer at the (Atop) Adsorption Sites of the Pt(111) (p(2 × 2) Arrangement) and Pt(533) Surfaces, as Indicated in Figure 5a[c]

	monomer Pt(111)	monomer/Pt(533)				chain/ Pt(533)	
		site 1	site 2	site 3	site 4	mol. a	mol. b
E_{ads} (eV)	0.204	0.382	0.332	0.241	0.188	0.528	0.528
E_{ads}^0(eV)	0.153	0.317	0.265	0.180	0.137	0.442	0.442
$\angle_{HOH}$	105°	106°	103°	105°	105°	106°	104°
d_{O-H} (Å)	0.98	0.98	0.98	0.98	0.98	0.98/1.01	0.99
						1.66/2.58[a]	1.66/2.58[a]
d_{Pt-O} (Å)	2.58	2.43	3.23/2.50[b]	2.46	2.58	2.27	3.17

[a] Neighboring water molecules, which differ in adsorption height by 0.9 Å, are interlinked by hydrogen bonds with bond lengths of alternatively 1.66 and 2.58 Å. [b] Distances refer to the Pt atoms in the lower and upper terrace, respectively. [c] Results for a H_2O molecule involved in a molecular chain adsorbed at the upper side of steps of the Pt(533) surface are also presented. Compiled are the opening angle of the water molecule ($\angle_{HOH}$) and the O−H (d_{O-H}) and Pt−O distances (d_{Pt-O}) in Å.

TABLE 3: Adsorption Energies Per Adsorbate without (E_{ads}) and with Zero-Point Corrections (E_{ads}^0) for OH and H at the (Atop) Adsorption Sites of the Pt(533) Surface, as Indicated in Figure 6[b]

	OH/Pt(533)				H/ Pt(533)			
	site 1	site 2	site 3	site 4	site 1	site 2	site 3	site 4
E_{ads} (eV)	−0.565	−0.942	−0.959	−0.982	0.490	0.571	0.497	0.454
E_{ads}^0(eV)	−0.453	−0.837	−0.860	−0.870	0.453	0.532	0.443	0.401
$\angle_{surf-OH}$	52°	36°	59°	60°				
d_{O-H} (Å)	0.98	0.98	0.98	0.98				
$d_{Pt-O/H}$ (Å)	1.96	2.11/2.05[a]	2.00	2.02	1.57	1.73	1.56	1.56

[a] Distances refer to the Pt atoms in the lower and upper terrace, respectively. [b] The adsorption energy for OH is given with respect to the energy difference of a free water molecule and half that of a free hydrogen molecule, for hydrogen half the free molecule is taken as reference. Compiled are the angle between the macroscopic surface normal and the OH axis, ($\angle_{surf-OH}$), and the O−H (d_{O-H}) and Pt− O/H distances ($d_{Pt-O/H}$) in Å.

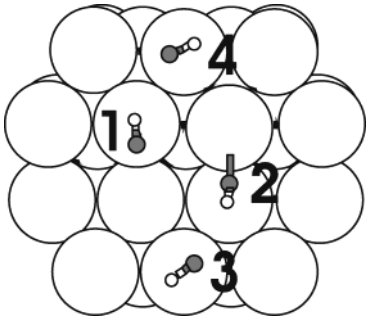

Figure 6. Top view of the atop adsorption sites of OH on the Pt(533) surface. The numbering scheme of the adsorption positions corresponds to that of Table 3, where adsorption energies and geometries are compiled.

adsorption geometry are compiled in Table 3. For illustrating the tilted adsorption geometry of OH, a sketch is shown in Figure 6.

The adsorption energies are given with respect to the free hydrogen molecule for H and for the difference between a free water molecule and half the energy of a free H_2 molecule for OH. This reference of quite stable molecules in the gas phase results in endothermic (negative) adsorption energies for OH in all configurations, again with a strong preference for the site at the upper step edge (site 1 in Figure 6). The hydrogen atom exhibits much less preference for various adsorption positions. The adsorption energy varies across the surface by less than 150 meV, indicative for low diffusion barriers. The adsorption energy is slightly more than 0.5 eV, just enough to compensate for the endothermic adsorption energy of the hydroxyl group. The sum of the adsorption energies, which corresponds to the energy balance of a dissociative adsorption of water, is for the most favorable configuration (OH in site 1, H at site 2) slightly above zero ($E = 0.079$ eV). However, the adsorption of intact water (Table 2) appears to be 200 meV more stable than the dissociative adsorption of water on the steps of Pt(533). Hence, it follows from the DFT calculations that dissociative adsorption of water is energetically unfavorable. Our calculations do not include the effect of hydrogen bonding on the energetics of water dissociation, for reasons of limited computational power. However, the dissociation of water on transition- and noble-metal surfaces has recently been shown to depend mainly on the OH-metal bond strength in the final state and to a much lesser extent on hydrogen bonding.[63]

To unravel the stabilization of water as molecular chains, the energetics of formation of such a molecular chain was investigated. The adsorption energy of a "single" H_2O molecule that is part of a molecular chain adsorbed along the step edge (illustrated in Figure 5b) is also given in Table 2. In agreement with the experimental data, the calculated adsorption energies (Figure 5, Table 2) indicate a very substantial (∼40%) stabilization of water adsorbed as a molecular chain on the step sites of Pt(533). Neighboring water molecules, which differ in adsorption height by 0.9 Å, are interlinked by hydrogen bonds with bond lengths of alternatively 1.66 and 2.58 Å. The hydrogen bond length of 2.58 Å predicted by the DFT calculation is apparently large in comparison with the experimental values found for O−H···O bonds in solids.[64] So, the configuration of water adsorbed on metal surfaces continues to create controversies; several discrepancies reported between LEED experiments[65,66] and DFT calculations[5,6] are also still unanswered. In any case, the molecular geometry is still almost gas-phase-like; only the hydrogen bonds of unequal strength lead to a slightly asymmetric stretching of the OH bonds. Remarkably, the adsorption height of the lower water molecule within the chain is even lower than that of the isolated monomer.

For coverages between 0 and 0.33 ML (Figure 1 (top panel)), the intensity of the 198 K peak continues to increase as the water coverage increases. Around the same coverage (up to 0.39 ML), the intensity of the 3318 cm^{-1} peak in the RAIRS spectra (Figure 4 (left panel), curves a−c) continuously increases, although the line shape remains unchanged. Given both the significant diffusivity and clustering ability of water on the Pt surface at 100 K, we can ascribe the 198 K peak to water desorbing from structures originating from the steps. The coverage at which the additional 185 K peak appears in the TPD is higher than one would expect for full coverage of the steps. However, STM measurements on step-decorated Pt(111) surface[21] have previously demonstrated that the molecular chains may have a width larger than one molecule, depending on the precise step geometry.

At coverages exceeding 0.33 ML, a new type of desorption site is observed in the water TPD spectra (Figure 1 (top panel) and (middle panel)). As the step sites are expected to be fully occupied at $\Theta = 0.25$, the new peak at 185 K must correspond to water desorption from (111) terrace sites of Pt(533) surface. It is likely that the water structures desorbing at ∼185 K appear because of extension of the water cluster from the steps onto the terraces, in contrast to independent nucleation of water islands on the terraces. STM experiments[21] have indeed shown that water molecules in the two-dimensional islands grown out from the lower side of the step edges have a lower binding energy than water at the steps. Although the water molecules in these islands are adsorbed more weakly than those at the steps, they are bonded more strongly than on the Pt(111) surface: the desorption temperature (185 K) indicates an additional stabilization of water on terraces because of water on the step sites, compared to the situation of CO saturated steps, which results in a desorption temperature (∼175 K, Figure 3) comparable to that from the Pt(111) surface.

3.2. The Multilayer Regime. Figure 7 depicts TPD spectra (rate: 2 Ks^{-1}) of water multilayers grown on Pt(533) at 100 K. Similar behavior was observed for heating rates of 4 and 6 Ks^{-1}. One peak corresponding to overlayer desorption can be observed

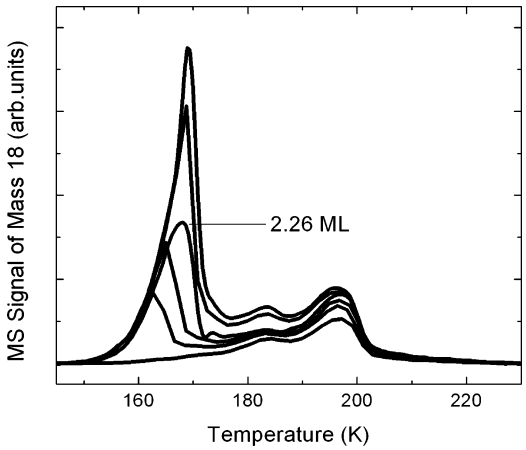

Figure 7. TPD spectra of H_2O dosed at $T_S = 100$ K on Pt(533). Water dosing rate was 0.01 MLs^{-1}. The (multilayer) coverages (in ML, computed on the basis of peak integrated areas) are, from bottom to top, 1.08, 1.64, 2.06, 2.26, 3.25, and 3.76. Heating rate was 2 Ks^{-1}.

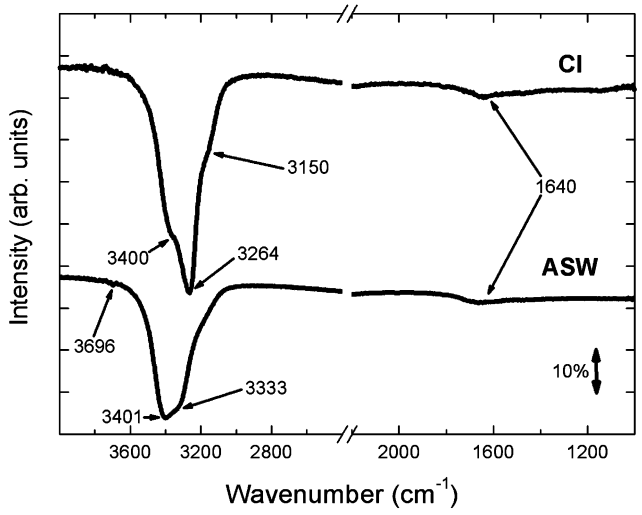

Figure 8. RAIR spectra of ~40 ML of amorphous solid water (lower trace) and crystalline ice (upper trace) films, shown in the frequency ranges of 4000−2400 and 2200−1000 cm^{-1}.

at 160 K, which shifts to higher temperatures and does not saturate with increasing exposure. At very high coverages (≥40 ML), not shown here, this peak dominates the spectrum and obscures monolayer desorption.

The desorption features of water multilayers from Pt(533) are very similar to those reported for Pt(111), with small variations of the desorption temperature[11−14,24,26,27] (see Table 1). Multilayer ice desorption from Pt(100), measured under conditions of a very high TPD rate (12−16 Ks^{-1}), occurs at slightly lower temperatures, in the range of 150−155 K.[29,30] Not surprisingly, the influence of the stepped character of our Pt surface on the desorption of water decreases significantly once the first monolayer is saturated.

Although most of the traces in Figure 7 have a common leading edge for the multilayer desorption peak (which is typical for zero-order desorption kinetics), the 2.26 ML trace exhibits a small but significant shift (to higher temperature) of the leading edge of the multilayer peak. The shift is visible regardless of heating rate (2−6 Ks^{-1}) and can be associated with the heating-induced reordering of the first deposited water layers, as has been observed previously on Pt(111).[24]

Figure 8 depicts the RAIR spectra of ~40 ML thick amorphous solid water (grown at 100 K, by employing a high water beam flux — ~0.06 MLs^{-1}) and crystalline ice (obtained by annealing to 145 K an initially amorphous solid water film) films on the Pt(533) surface. The spectral domain is split into two parts that exhibit characteristic H_2O vibrational frequencies: the OH bending mode region (~1590−1640 cm^{-1}) and the OH stretching mode region (~3000−3700 cm^{-1}). A similar crystalline ice RAIR spectrum can be obtained for crystalline ice grown directly by water adsorption at 145 K.

Similar to the water layer grown on Pt(111), the RAIR spectrum of amorphous solid water (Figure 8) on Pt(533) is broad and rather featureless in the 3000−3690 cm^{-1} range and has a small and sharp feature at 3696 cm^{-1}, attributed to the stretching mode of free OH groups on the ice surface (non-H-bonded, dangling O−H bonds).[67] Two differences between the spectra of amorphous and annealed layers are apparent: first, the change of the rather broad region of ASW into three distinct features, at 3400, 3264, and 3150 cm^{-1}, consistent with crystallization of the amorphous phase. Second, the intensity of the free OH peak at 3696 cm^{-1} is reduced during the crystallization process, in agreement with the low ratio (approximately one to six) estimated between the number of free OH groups on the surface of crystalline and amorphous ice.[68]

4. Conclusions

TPD measurements of water desorbing from Pt(533) reveal two submonolayer desorption states and one feature corresponding to a multilayer desorption state. The multilayer feature is similar to that observed for water desorption from a flat Pt(111) surface, while for a submonolayer coverage the (100) steps induce an additional stabilization of water adsorbed on the Pt(533) surface. At coverages ($\Theta > 0.33$ ML) exceeding that for which the steps are fully occupied ($\Theta = 0.25$ ML), desorption features appear at lower temperatures, corresponding to water desorbing from the terraces. The H_2O uptake curve indicates a coverage-independent sticking coefficient of 1 on both the bare Pt and ice-covered surfaces.

RAIRS results show the H-bonding of water molecules already at very low coverage (≤0.05 ML). The preference of water molecules to associate in molecular chains along the step edges of the Pt(533) surface concluded from the combination of TPD and RAIRS results is confirmed by the DFT calculations of adsorption energetics. In addition, both RAIRS and DFT results indicate adsorption of intact H_2O on Pt(533), although we cannot rule out some dissociation.

Similar to observations on the Pt(111) substrate, RAIRS investigations of water multilayers grown on Pt(533) show important differences between amorphous solid water and crystalline ice surfaces in free OH fraction and implicitly in hydrogen bond ability. This implies a different surface chemical behavior of amorphous solid water and crystalline ice films grown on Pt(533) substrate in subsequent interactions with potential adsorbates.[69]

Acknowledgment. This work is part of the research program of the Foundation for Fundamental Research on Matter (FOM), which is financially supported by The Netherlands Organization for Scientific Research (NWO). We gratefully thank the Royal Dutch Academy of Arts and Sciences (KNAW) for additional financial support.

References and Notes

(1) Henderson, M. A. *Surf. Sci. Rep.* **2002**, *46*, 1.
(2) Thiel, P. A.; Madey, T. E. *Surf. Sci. Rep.* **1987**, *7*, 211.
(3) Ludwig, R. *Angew. Chem., Int. Ed.* **2003**, *42*, 3458.
(4) Denzler, D. N.; Hess, C.; Dudek, R.; Wagner, S.; Frischkorn, C.; Wolf, M.; Ertl, G. *Chem. Phys. Lett.* **2003**, *376*, 618.

(5) Feibelman, P. J. *Science* **2002**, *295*, 99.
(6) Michaelides, A.; Alavi, A.; King, D. A. *J. Am. Chem. Soc.* **2003**, *125*, 2746.
(7) Clay, C.; Haq, S.; Hodgson, A. *Chem. Phys. Lett.* **2004**, *388*, 89.
(8) Ogasawara, H.; Brena, B.; Nordlund, D.; Nyberg, M.; Pelmenschikov, A.; Pettersson, L. G. M.; Nilson, A. *Phys. Rev. Lett.* **2002**, *89*, 276102.
(9) Meng, S.; Xu, L. F.; Wang, E. G.; Gao, S. *Phys. Rev. Lett.* **2002**, *89*, 176104.
(10) Fischer, G. B.; Gland, J. L. *Surf. Sci.* **1980**, *94*, 446.
(11) Jo, S. K.; Kiss, J.; Polanco, J. A.; Whites, J. M. *Surf. Sci.* **1991**, *253*, 233.
(12) Panja, C.; Saliba, N.; Koel, B. E. *Surf. Sci.* **1998**, *395*, 248.
(13) Su, X.; Lianos, L.; Shen, Y. R.; Somorjai, G. A. *Phys. Rev. Lett.* **1998**, *80*, 1533.
(14) Ogasawara, H.; Yoshinobu, J.; Kawai, M. *Chem. Phys. Lett.* **1994**, *231*, 188.
(15) Nakamura, M.; Shingaya, Y.; Ito, M. *Chem. Phys. Lett.* **1999**, *309*, 123.
(16) Ogasawara, H.; Yoshinobu, J.; Kawai, M. *J. Chem. Phys.* **1999**, *111*, 7003.
(17) Sexton, B. A. *Surf. Sci.* **1980**, *94*, 435.
(18) Jacobi, K.; Bedürftig, K.; Wang, Y.; Ertl, G. *Surf. Sci.* **2001**, *472*, 9.
(19) Glebov, A. L.; Graham, A. P.; Menzel, A. *Surf. Sci.* **1999**, *427/428*, 22.
(20) Starke, U.; Heinz, K.; Materer, N.; Wander, A.; Michl, M.; Döll, R.; Hove, M. A. V.; Somorjai, G. A. *J. Vac. Sci. Technol. A* **1992**, *10*, 2521.
(21) Morgenstern, M.; Michely, T.; Comsa, G. *Phys. Rev. Lett.* **1996**, *77*, 703.
(22) Schmitz, P. J.; Polta, J. A.; Chang, S.-L.; Thiel, P. A. *Surf. Sci.* **1987**, *186*, 219.
(23) Glebov, A. L.; Graham, A. P.; Menzel, A.; Toennies, J. P. *J. Chem. Phys.* **1997**, *106*, 9382.
(24) Haq, S.; Harnett, J.; Hodgson, A. *Surf. Sci.* **2002**, *505*, 171.
(25) Souda, R. *J. Phys. Chem. B* **2001**, *105*, 5.
(26) Gilarowski, G.; Erley, W.; Ibach, H. *Surf. Sci.* **1996**, *351*, 156.
(27) Biener, J.; Lang, E.; Lutterloh, C.; Küppers, J. *J. Chem. Phys.* **2002**, *116*, 3063.
(28) Daschbach, J. L.; Peden, B. M.; Smith, R. S.; Kay, B. D. *J. Chem. Phys.* **2004**, *120*, 1516.
(29) Kizhakevariam, N.; Stuve, E. M. *J. Vac. Sci. Technol. A* **1990**, *8*, 2557.
(30) Kizhakevariam, N.; Stuve, E. M. *Surf. Sci.* **1992**, *275*, 223.
(31) Hoffmann, W.; Benndorf, C. *Surf. Sci.* **1997**, *377*−*379*, 681.
(32) Hoffmann, W.; Benndorf, C. *J. Vac. Sci. Technol. A* **2000**, *18*, 1520.
(33) Miller, J. N.; Lindau, I.; Spicer, W. E. *Surf. Sci.* **1981**, *111*, 595.
(34) Skelton, D. C.; Tobin, R. G.; Fisher, G. B.; Lambert, D. K.; DiMaggio, C. L. *J. Phys. Chem. B* **2000**, *104*, 548.
(35) Riedmüller, B.; Giskes, F.; Loon, D. G. v.; Lassing, P.; Kleyn, A. W. *Meas. Sci. Technol.* **2002**, *13*, 141.
(36) Jenniskens, H. G.; Bot, A.; Dorlandt, P. W. F.; Essenberg, W. v.; Haas, E. v.; Kleyn, A. W. *Meas. Sci. Technol.* **1997**, *8*, 1313.
(37) Wang, H.; Tobin, R. G.; DiMaggio, C. L.; Fisher, G. B.; Lambert, D. K. *J. Chem. Phys.* **1997**, *107*, 9569.
(38) Smith, R. S.; Dohnálek, Z.; Kimmel, G. A.; Stevenson, K. P.; Kay, B. D. *Chem. Phys.* **2000**, *258*, 291.
(39) Kresse, G.; Furthmüller, J. *Phys. Rev. B* **1996**, *54*, 11169.
(40) Kresse, G.; Furthmüller, J. *Comput. Mat. Sci.* **1996**, *6*, 15.
(41) http://cms.mpi.univie.ac.at/vasp/.
(42) Kresse, G.; Joubert, D. *Phys. Rev. B* **1998**, *59*, 1758.
(43) Perdew, J. P.; Chevary, J. A.; Vosko, S. H.; Jackson, K. A.; Pederson, M. R.; Singh, D. J.; Fiolhais, C. *Phys. Rev. B* **1992**, *46*, 6671.
(44) Brown, D. E.; George, S. M.; Huang, C.; Wong, E. K. L.; Rider, K. B.; Smith, R. S.; Kay, B. D. *J. Phys. Chem.* **1996**, *100*, 4988.
(45) Smith, R. S.; Kay, B. D. *Surf. Rev. Lett.* **1997**, *4*, 781.
(46) Braun, J.; Glebov, A.; Graham, A. P.; Menzel, A.; Toennies, J. P. *Phys. Rev. Lett.* **1998**, *80*, 2638.
(47) At 100 K, CO is adsorbed preferentially on the step sites of Pt surface,[48−50] while the adsorption site of water adsorbed at this temperature on the terrace sites has been demonstrated to be unaffected by coadsorbed CO.[16]
(48) Hayden, B. E.; Kretzschmar, K.; Bradshaw, A. M.; Greenler, R. G. *Surf. Sci.* **1985**, *149*, 394.
(49) Luo, J. S.; Tobin, R. G.; Lambert, D. K.; Fisher, G. B.; DiMaggio, C. L. *Surf. Sci.* **1992**, *274*, 53.
(50) Roke, S.; Coquel, J. M.; Kleyn, A. W. *J. Chem. Phys.* **2000**, *113*, 6376.
(51) Wagner, F. T.; Moylan, T. E.; Schmieg, S. J. *Surf. Sci.* **1988**, *195*, 403.
(52) Ibach, H.; Lehwald, S. *Surf. Sci.* **1980**, *91*, 187.
(53) Baumann, P.; Pirug, G.; Reuter, D.; Bonzel, H. P. *Surf. Sci.* **1995**, *335*, 186.
(54) Bensebaa, F.; Ellis, T. H. *Prog. Surf. Sci.* **1995**, *50*, 173.
(55) Clay, C.; Haq, S.; Hodgson, A. *Phys. Rev. Lett.* **2004**, *92*, 046102.
(56) Karlberg, G. S.; Olsson, F. E.; Persson, M.; Wahnstrom, G. *J. Chem. Phys.* **2003**, *119*, 4865.
(57) Smoluchowski, R. *Phys. Rev.* **1941**, *60*, 661.
(58) Materer, N.; Starke, U.; Barbieri, A.; Hove, M. A. v.; Somorjai, G. A.; Kroes, G. J.; Minot, C. *Surf. Sci.* **1997**, *381*, 190.
(59) Michaelides, A.; Ranea, V. A.; Andres, P. L. d.; King, D. A. *Phys. Rev. Lett.* **2003**, *90*, 216102.
(60) Stair, P. C. *J. Am. Chem. Soc.* **1982**, *104*, 4044.
(61) Santen, R. A. v.; Neurock, M. *Catal. Rev.*−*Sci. Eng.* **1995**, *37*, 557.
(62) Michaelides, A.; Hu, P. *J. Am. Chem. Soc.* **2001**, *123*, 4235.
(63) Michaelides, A.; Alavi, A.; King, D. A. *Phys. Rev. B* **2004**, *69*, 113404.
(64) Pimentel, G. C.; McClellan, A. L. *The Hydrogen Bond*; W. H. Freeman and Company: San Francisco, 1960.
(65) Puisto, S. R.; Lerotholi, T. J.; Held, G.; Menzel, D. *Surf. Rev. Lett.* **2003**, *10*, 487.
(66) Held, G.; Menzel, D. *Surf. Sci.* **1994**, *316*, 92.
(67) Buch, V.; Devlin, J. P. *J. Chem. Phys.* **1991**, *94*, 4091.
(68) Schaff, J. E.; Roberts, J. T. *J. Phys. Chem.* **1996**, *100*, 14151.
(69) Grecea, M. L.; Backus, E. H. G.; Fraser, H. J.; Pradeep, T.; Kleyn, A. W.; Bonn, M. *Chem. Phys. Lett.* **2004**, *385*, 244.